Pergamon

PII: S0191–8141(98)00016–9

Journal of Structural Geology, Vol. 20, No. 7, pp. 841 to 856, 1998

0191-8141/98 $19.00 + 0.00

Geometry, mechanisms and significance of extensional folds from examples in the Rocky Mountain Basin and Range province, U.S.A.

SUSANNE U. JANECKE*, COLBY J. VANDENBURG and JAMES J. BLANKENAU

Department of Geology, Utah State University, Logan, UT 84322-4505, U.S.A.

(*Received* 21 *July* 1997; *accepted in revised form* 17 *February* 1998)

Abstract—Geologic mapping and structural analysis in Paleogene half graben of Idaho and Montana have revealed over 70 extensional folds that form orthogonal sets with mostly NE- and SE-trending axes. On a regional scale they parallel or lie perpendicular to the strikes of the largest normal faults. Transverse folds, at a high angle to the fault, and folds oblique to the fault, comprise more than half of the folds and reflect the highly three-dimensional nature of the bulk strain. Detailed geometric analysis of 15 folds in the Salmon, Horse Prairie and Medicine Lodge basins shows that they typically have an upright to steeply inclined bisecting surface, an interlimb angle of 141°, and a plunge of 19°.

Based on our synthesis of the eight common mechanisms of extensional folding and their distinguishing characteristics, we were able to determine how some of the investigated folds formed. Fault-bend folding above both fault-parallel and fault-perpendicular bends in the underlying normal fault produced most of the folds in the study area, but displacement gradients along normal faults, fault-drag, isostatic adjustments, and transtension were also factors in the deformation. Most of the compound folds, which result from more than one mechanism of folding, are oblique to all adjacent normal faults. Recognition of such extensional folds is critical, because they might be misinterpreted as contractional structures, they influence sediment thickness patterns and dispersal in rift basins, and may control the migration and trapping of petroleum and groundwater resources. © 1998 Elsevier Science Ltd. All rights reserved

INTRODUCTION

With the exception of rollover folds (Hamblin, 1965; Groshong, 1989, 1994; Dula, 1991; Xiao and Suppe, 1992), folds are thought to be relatively rare in extensional settings (Twiss and Moores, 1992; Davis and Reynolds, 1996). The view that folds require contraction is at odds with relationships in the Rocky Mountain Basin and Range province (see below) and with dozens of studies documenting folds in extensional settings from around the world (Schlische, 1995; and localities in Fig. 1). Extensional folds occur throughout the Basin and Range province, in accommodation zones, metamorphic core complexes, regions of both modest and large-magnitude extension, the Rio Grande rift, zones of constriction, transtension, and plane strain extension (Fig. 1) (Spencer, 1984; John, 1987; Stewart and Diamond, 1990; Bartley *et al.*, 1990; Yin and Dunn, 1992; Anderson and Barnhard, 1993a,b; Russell and Snelson, 1994; Lewis and Baldridge, 1994; Holm *et al.*, 1994; Mancktelow and Pavlis, 1994; Faulds and Varga, in press; Fowler *et al.*, 1995; Olson, 1996; Kruger *et al.*, 1995; Faulds, 1996; Howard and John, 1997). Although many recent studies have described extensional folds, their geometry is rarely quantified, their significance is under-appreciated, and their origin is incompletely understood.

In order to assess the processes of extensional folding responsible for more than a dozen folds in our study area in Montana and Idaho, U.S.A., we analyze their geometry, summarize the mechanisms of extensional folding, and provide criteria to distinguish among them. This synthesis of mechanisms expands on a benchmark paper by Schlische (1995) which detailed the geometries and origins of fault-related folds in extensional settings from around the world. We revisit Schlische's classification because constrictional, transtensional, and isostatic folds were not considered in Schlische's paper. Furthermore, analogy with contraction indicates that the kinematics and mechanics of fault-drag, forced, and fault-propagation folds differ and should be treated separately (e.g. Twiss and Moores, 1992).

Schlische (1995) used the term longitudinal and transverse to describe folds that lie parallel or perpendicular to the associated normal fault. Although many folds appear to fall into these two categories, folds with axes oblique to normal faults are also common (Table 1). We use the term oblique to describe any fold with a trend that is between 22.5° and 67.5° from the strike of the associated normal fault. Longitudinal and transverse folds are defined as having trends within 22.5° from strike parallel or strike perpendicular. Because only one folding process, fault-bend folding, is capable of producing folds of any orientation (Table 1), classifying a fold as longitudinal, transverse, or oblique greatly limits the possible mechanisms of folding, whenever one mechanism produced the folding.

In order to illustrate the diversity and significance of extensional folds, we present results of our field studies

*e-mail: sjanecke@cc.usu.edu

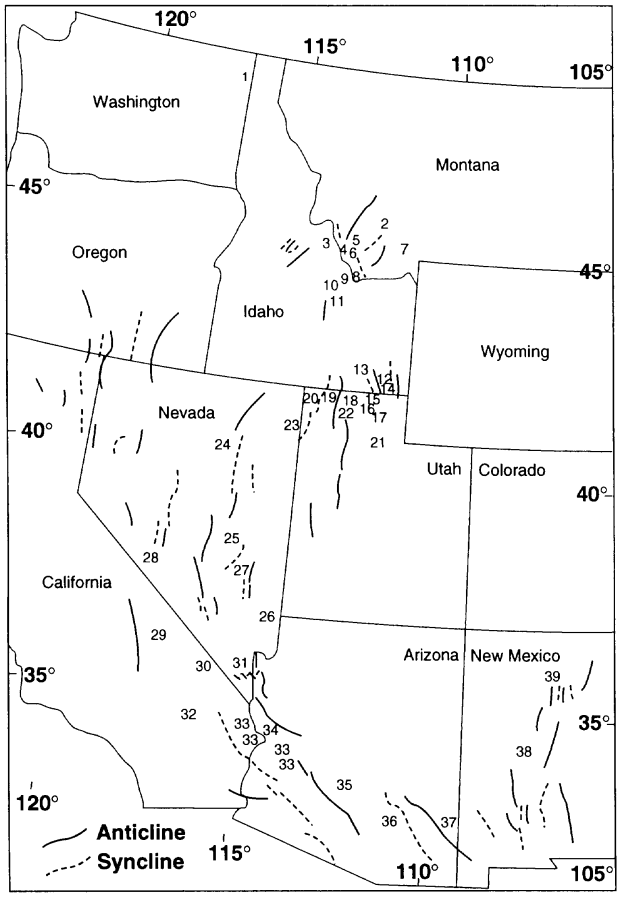

Fig. 1. Map showing the distribution of extensional folds in the Basin and Range province, U.S.A. Locations of anticlinal and synclinal tilt-domain boundaries in the Basin and Range province were modified from Stewart *et al.* (in press). Sources of data are given in the Appendix.

in the Rocky Mountain Basin and Range province and analyze the geometries of 15 selected folds in detail. We identify the mechanisms that produced eight of them, and briefly discuss the possible origins of the other seven before considering the overall significance of such structures. Additional examples of extensional folds are in Schlische (1995) and the papers cited in the Appendix.

GEOMETRY OF EXTENSIONAL FOLDS IN ROCKY MOUNTAIN BASIN AND RANGE PROVINCE

Extensional folds in the Grasshopper, Horse Prairie, Medicine Lodge, Muddy Creek, and Salmon half graben of SW Montana and eastern Idaho are closely associated with a complex array of normal or normal-oblique slip faults (Figs 2 & 3) (M'Gonigle and Dalrymple, 1993, 1996; Janecke *et al.*, 1996a; M'Gonigle and Hait, 1997; VanDenburg, 1997; VanDenburg *et al.*, in press; Blankenau and Janecke, 1997; Janecke *et al.*, in press). The five half graben formed in the Eocene to early Miocene, after the end

Table 1. Mechanisms that produce folds in extensional settings. Letters refer to Fig. 8

Longitudinal (fault parallel ±22.5°)	Transverse (fault-perpendicular ±22.5°)	Oblique (22.5–67.5° to fault)
A. Isostatic folds	E. Fault-bend folds	Fault-bend folds
B. Fault-bend folds*	F. Constrictional folds	Transtensional folds
C. Fault-propagation folds	G. Displacement-gradient folds	Compound folds
D. Fault-drag folds	Compound folds	
Compound folds		

*A resulting anticline is usually termed a rollover and reverse-drag fold.

of Laramide and Sevier contractional deformation in the early Tertiary. More than 70 extensional folds were identified during geologic mapping of the syntectonic basin-fill deposits and some were also imaged on seismic reflection profiles acquired in the early 1980s by Sohio Oil Company and donated by Enserch Exploration (S. Janecke, unpublished data). Several generations of extensional folds are genetically related

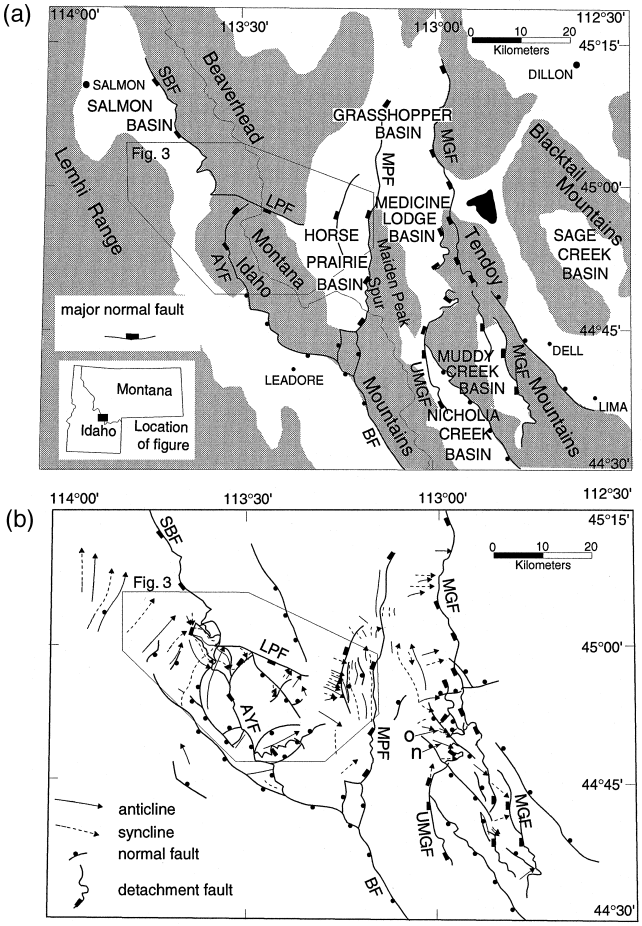

Fig. 2. (a) Index map of Paleogene rift basins in southwest Montana and eastern Idaho showing the major detachment faults. SBF = Salmon basin detachment fault, AYF = Agency–Yearian fault, MPF = Maiden Peak fault, MGF = Muddy-Grasshopper detachment fault, UMGF = upper detachment fault of Muddy-Grasshopper fault system, and BF = Beaverhead fault. (b) Simplified map showing extensional folds and normal faults in the region at the same scale as (a). Compiled from sources at locations 3–8 in the Appendix. n, o show the locations of folds in Fig. 4.

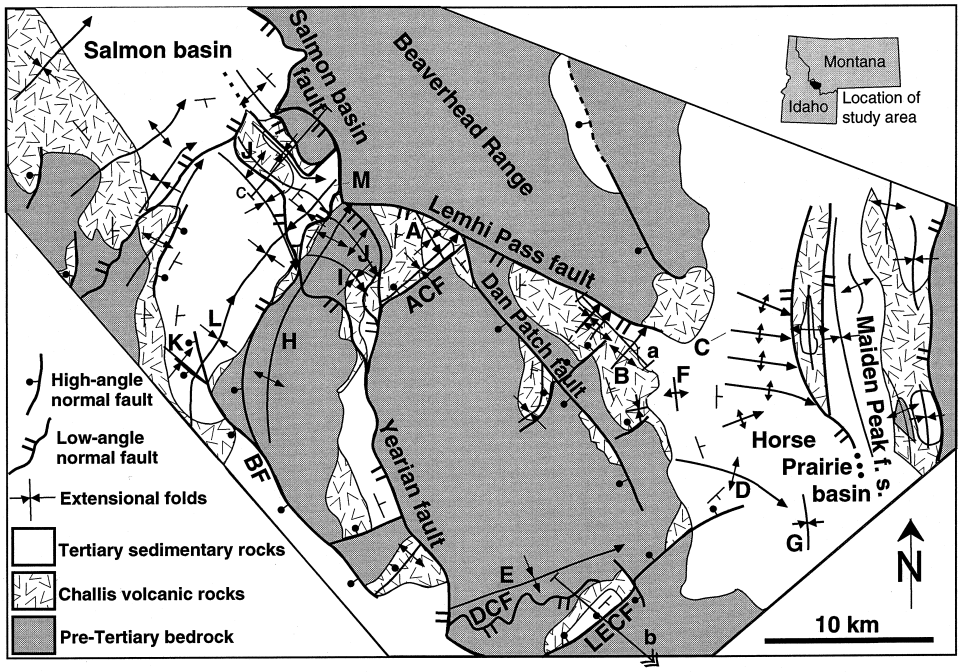

Fig. 3. Simplified geologic map of extensional folds in part of the study area. Location shown in Fig. 2. Located at 3 and 4 in Fig. 1. Geometric data for named folds is given in Fig. 4. Note that the synclines in the train of folds parallel to fold C were omitted for clarity. Compiled from sources at locations 3 and 5 in the Appendix.

to several generations of normal faults that extended the study area in both NE–SW and NW–SE directions during the Cenozoic (Fig. 2). With the possible exception of two small faults, thrust or reverse faults of middle Eocene to Miocene age are lacking from the study area. Normal faults, in contrast, are abundant, have a variety of orientations, and many have several kilometers of dip-slip separation across them. Except along the right-normal slip Lemhi Pass fault (VanDenburg *et al.*, in press) we infer that dip slip greatly exceeds strike slip across most of the faults. This is based on the presence of thick syntectonic basin-fill in the hanging walls of many faults and slickenlines on subsidiary faults in the footwall of the Salmon basin and Muddy-Grasshopper detachment faults. Cross-cutting relationships and local growth strata show that folds are coeval with the associated normal faults and formed between middle Eocene and early Miocene time. The presence of large numbers of transverse and oblique folds (Fig. 2) argues against formation of the folds in a fold and thrust belt, where longitudinal folds dominate in high strain regions.

On a regional scale, the trends of extensional folds are clearly related to the strikes of the largest normal faults (Fig. 2b). In the Grasshopper and Medicine Lodge half graben, folds trend roughly N–S and E–W in the hanging wall of the W- to WSW-dipping Muddy-Grasshopper and Maiden Peak detachment systems (Fig. 2). Farther to the west where the largest normal faults have a SW-dip direction and numerous NW-dipping cross faults are present, most extensional folds trend NE–SW and SE–NW (Figs 2 & 3). The transition between the eastern and western regions occurs in the Horse Prairie half graben, in the hanging wall of the Maiden Peak fault system (Figs 2b & 3). There is considerable variability in the geometries of folds, however, within each domain and along trend of individual folds. For example, folds H and M, a syncline–anticline pair, are probably both related to a ramp in the underlying NW- to W-dipping Agency-Yearian fault, yet they plunge in opposite directions, and their trends differ by about 40° (Figs 3 & 4). Syncline M probably extends to the SW as syncline L yet the plunge directions have reversed and the trends and plunges differ by 37° and 33°, over a distance of only 10 km (Figs 3 & 4). The orthogonality of the hingelines of folds that is so striking in Figs 2 and 3 is less apparent when the orientations of folds axes are compiled (Fig. 5).

Many folds in the study area are in fold trains (more than two parallel folds) with spacing that ranges from a low of 250 m (for some of the folds parallel to anticline C), to a high of 5 km (between anticline H and a syncline to the southeast) (Figs 3 & 2b). A single process cannot explain all these fold trains because some are at a high angle to the associated normal fault (folds parallel to anticline C; folds in the eastern Grasshopper basin, Fig. 2b), whereas others parallel the nearest normal faults (folds H, L, M and the syncline southeast of anticline H; anticline J and the adjacent synclines; folds in the eastern Horse Prairie basins between strands of the Maiden Peak fault zone) (Fig. 3).

Attitudes from the limbs of 15 extensional folds in the Horse Prairie, Salmon and Medicine Lodge half graben were analyzed to determine the orientations of

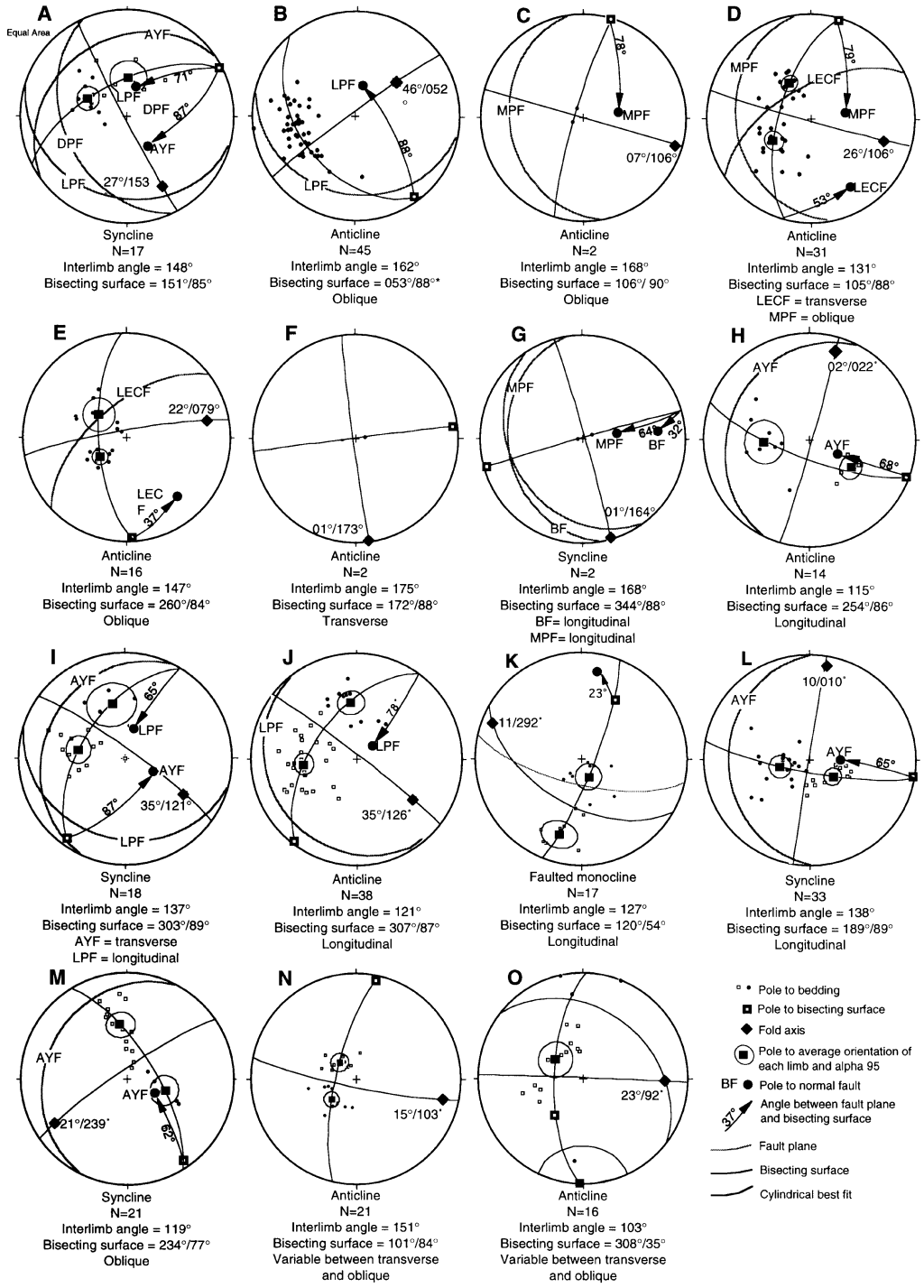

Fig. 4. Stereograms of poles to bedding for selected extensional folds in the Horse Prairie, Salmon and Medicine Lodge basins. See Figs 2 and 3 for locations of folds and associated faults. The data points conform well to a cylindrical model of fold form. Fold axes are defined by cylindrical best fit π great circles through poles to bedding within middle Eocene volcanic rocks, younger sedimentary rocks, and/or Proterozoic quartzites. Great circles depict near-surface attitudes of the associated normal faults and bisecting surfaces. Arrows indicate angular distance between each bisecting surface and associated normal fault. Mean poles to bedding and 95% confidence interval cones were calculated for individual limbs where possible. N = number of data points; DPF = Dan Patch fault; LPF = Lemhi Pass fault; MPF = Maiden Peak fault; LECF = Little Eightmile Creek fault; BF = Beaverhead fault; AYF = Agency-Yearian fault.

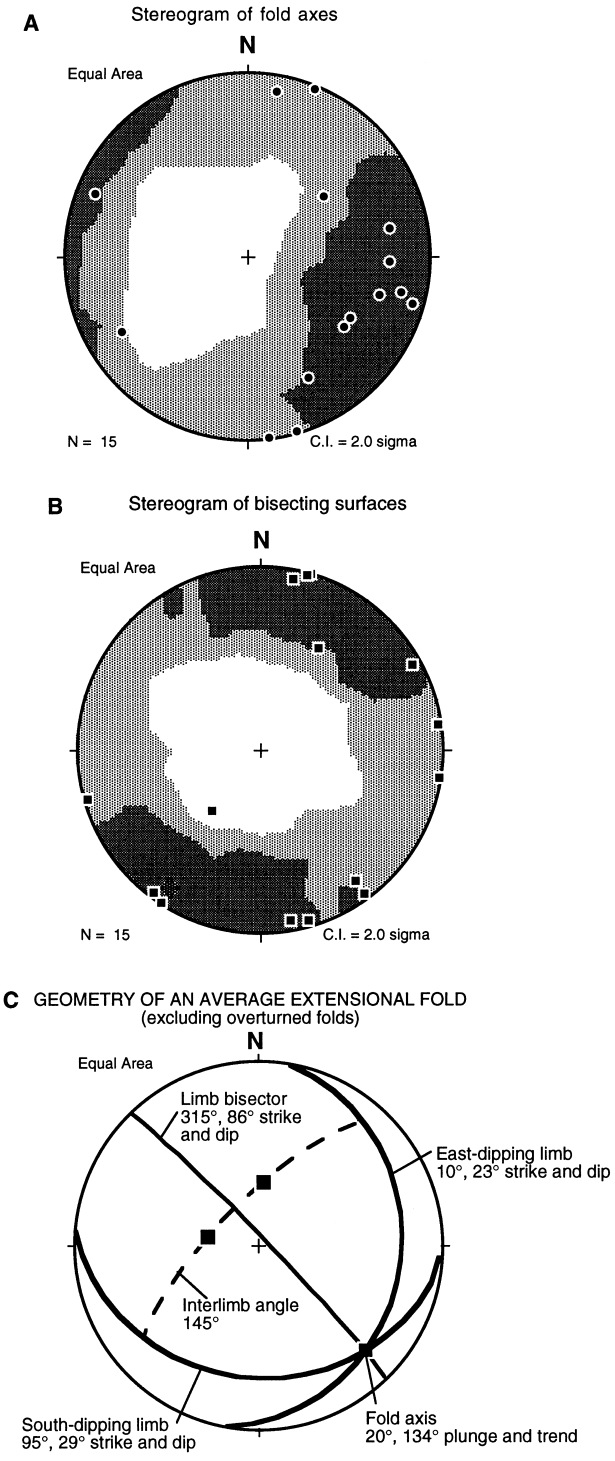

Fig. 5. Stereograms summarizing the fold axes (a) and bisecting surfaces (b) of the 15 selected folds in the study area (Fig. 4). An average fold is shown in (c). Folds typically have low plunges and subvertical bisecting surfaces, unless one limb is overturned.

their fold axes and bisecting surfaces, the interlimb angles, and the geometric relationship between folds and the associated normal fault(s) (Fig. 4). The geometric relationships between the extensional folds and genetically related normal faults are varied (Figs 3 & 4). Some folds have planar limbs with rounded hinges whereas others have smoothly varying forms (Fig. 6). Most folds appear to be harmonic, class one folds, based on reflection seismic data and exposures at different structural levels of plunging folds (Fig. 6). Interlimb angles, which were calculated by determining the average orientation of each limb of the fold, range from 103° up to 175° (open to gentle folds) and average 141° (Figs 4 & 5). Plunges of the folds range from 01° to 46° and average 19° (Figs 4 & 5). We used the bisecting surface of the fold limbs to approximate the orientation of the axial surfaces, which could not be measured directly in the field. Bisecting surfaces vary tremendously in their strike but are uniformly steep and nearly vertical (Figs 4 & 5). Only folds K and O, which locally have overturned limbs, have bisecting surfaces that dip less than 77° (Fig. 4). If the overturned folds are excluded, the average dip of the bisecting surface is 86°. An 'average' fold constructed using the data in Fig. 4 (exclusive of the overturned folds) has limbs that dip 20–30° and an axis that plunges about 20° (Fig. 5). Most of the folds examined in this study are symmetric (Fig. 4).

Two small folds in the Medicine Lodge and Salmon half graben are noteworthy because they have locally overturned limbs (folds K and O, Figs 2, 4 & 7). Anticline O has the smallest interlimb angles of any fold in the study area (103°). In both folds one nearly flat to gently dipping limb is separated from a sub-vertical to overturned limb by a narrow hinge zone (Fig. 7). The origin of the overturned limbs in fold K and O is enigmatic but may be due to more than one deformational event. Comparisons with scaled physical models (Ellis and McClay, 1988) suggest that high competency contrasts within the folded sequence may also play a role in the development of steep to overturned fold limbs.

In the Horse Prairie half graben, where cross-cutting relationships show that at least three generations of folds are present, most of the folds developed during the most significant phase of extension (between middle Eocene and early Miocene, Phase 3 of VanDenburg, 1997; VanDenburg *et al.*, in press). Fold B, a NE-plunging anticline, is the oldest fold and formed early during phase 3 (Fig. 6a), whereas the ESE-plunging train of folds parallel to anticline C formed later during phase 3 (Fig. 3). Anticline E (Fig. 6b), and syncline G are even younger. The oldest folds in the Salmon basin, folds L, M, and H, are also part of a NE-trending train of folds (Blankenau and Janecke, 1997). Variations in the thickness of growth strata in fold M in the Salmon basin suggest that the NE-plunging folds (folds L, H and M) formed before the SE-trending anticline J (Fig. 6c) (Blankenau and Janecke, 1997). The superposition of two generations of folds with orthogonal trends results in a dome and basin structure in parts of the study area. This is most evident near the southeast end of syncline A, at the intersection of anticlines J and H, and along synclines L and M.

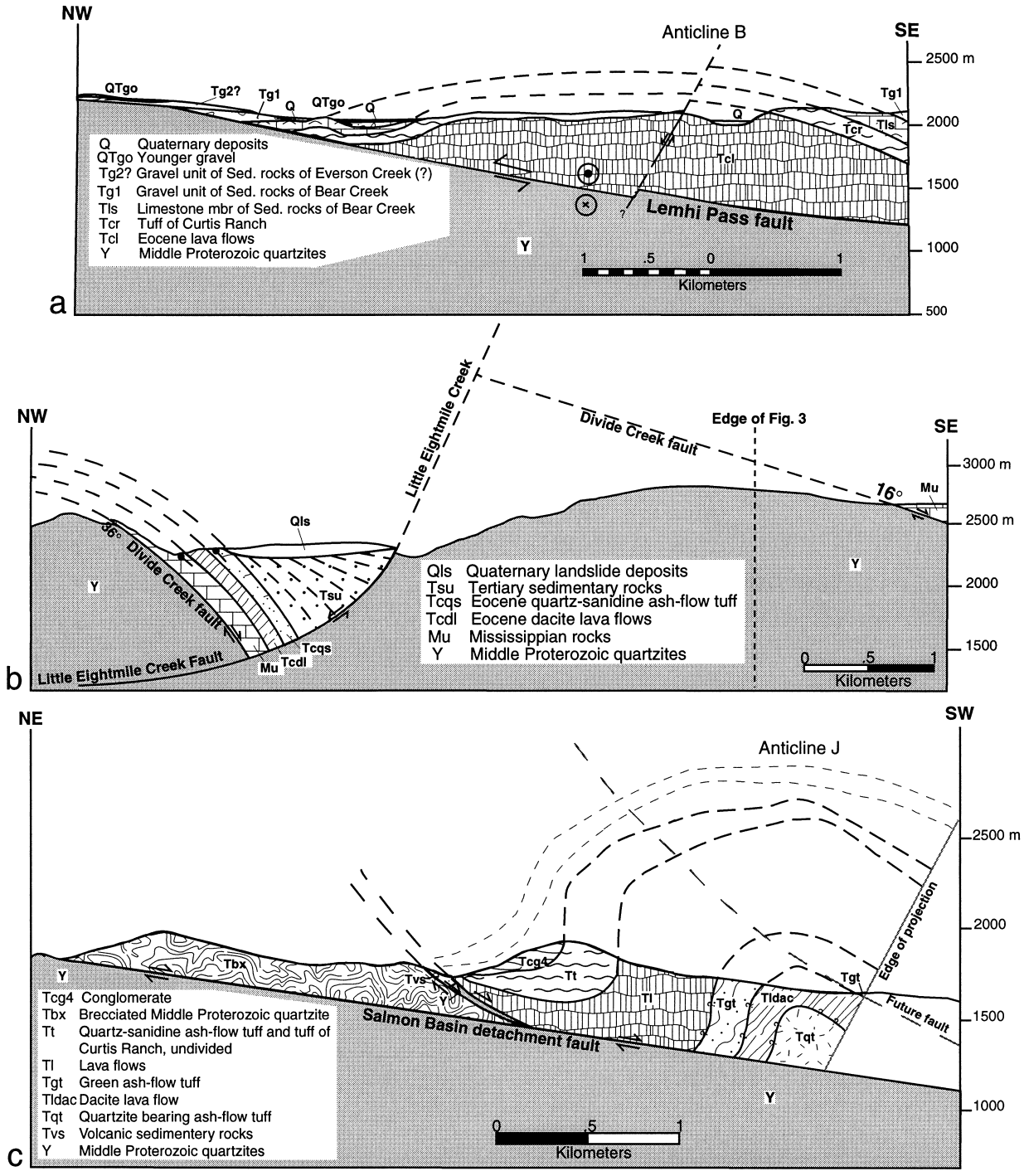

Fig. 6. (a) Cross-section of anticline B in the hanging wall of the Lemhi Pass fault. The component of apparent thrust slip on the Lemhi Pass fault is an artifact of the oblique line of cross-section relative to the normal-right slip fault. (b) Cross-section of anticline E showing fault-bend folding (rollover) of the older Divide Creek fault and overlying rocks in the hanging wall of the listric Little Eightmile Creek fault. Cross-cutting relationships demonstrate that folding postdates final slip on the Divide Creek fault (VanDenburg, 1997). (c) Down-plunge cross-section of anticline J. The fold axis of anticline J calculated in Fig. 4 and the method of Ramsay and Huber (1987) were used to generate the cross-section. This method produces an apparent view of adjacent structures because they do not have the same strike or trend as anticline J. Younger slip on the normal fault along the southwest flank of anticline J (future fault) was removed to reconstruct the cross-section. See Fig. 3 for locations of all three sections.

When we consider folds whose association with a particular fault is clear, 45% are oblique to the associated normal fault (Fig. 4). Similar results emerge when we qualitatively assign a geometric class to each of the other 72 extensional folds identified during our research in the Salmon, Horse Prairie, Grasshopper, Medicine Lodge, and Muddy Creek half graben. About 30% of the map traces of folds are oblique to the trace of the adjacent normal fault, about 45% are longitudinal and about 25% are transverse. The large numbers of oblique folds (trends between 22.5° and 67.5° to the strike of the associated normal fault) are puzzling because most of the mechanisms that we know of for producing extensional folds generate either longitudinal or transverse folds (Schlische, 1995; see below). An undocumented component of strike-slip deformation and/or multiple mechanisms of deformation could account for the large number of oblique folds in this area.

Extensional folds are major structural features in these rift basins and even control the basic outlines of some of the basins. In the Salmon half graben, for example, the irregular boundary between Tertiary and pre-Tertiary rocks along its southwest margin (Fig. 2) is due to several subbasin-scale N- to NE-plunging folds. Amplitudes of folds in the study area range up to 1.5 km (anticline H). The spacing of folds is irregular except in the fold train parallel to anticline C (Fig. 3). Orthogonal sets of folds occur both in areas dominated by a single geometric set of normal faults (e.g. Grasshopper half graben) and in areas where multiple generations of normal faults, some at high angles to one another, are present (Horse Prairie and Salmon half graben). The bulk strain recorded by the folds, like that recorded by the multiple sets of normal faults, is three-dimensional (VanDenburg *et al.*, in press; Blankenau and Janecke, 1997).

Many different mechanisms produced the folds in the study area. The need to better understand the origin of the extensional folds in the study area motivated our synthesis of the mechanisms of extensional folding presented below.

MECHANISMS THAT PRODUCE EXTENSIONAL FOLDS

Comparisons of the mechanisms that produce folds during contraction and analysis of the structural literature shows that more than a dozen distinct mechanisms (or processes) produce folds during extension. We will summarize those mechanisms that are relatively common and describe some of their distinguishing characteristics (Table 1 and Fig. 8). The terminology in Table 1 parallels the terminology used for contractional folds (e.g. Twiss and Moores, 1992) wherever possible and therefore differs somewhat from the terminology of Schlische (1995). We will consider longitudinal folds first and restrict our analysis to the most simple end-member cases.

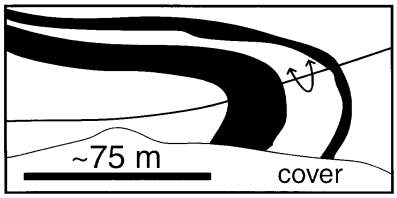

Fig. 7. Sketch of anticline O, an overturned fold in the Medicine Lodge half graben. View to the southeast. Black lines outline traces of bedding.

Longitudinal folds

Common longitudinal folds include isostatic folds, fault-bend folds (rollover folds), fault-propagation folds, and fault-drag folds (Table 1 and Fig. 8). Isostatic folds tend to be the largest, and fault-drag folds tend to be the smallest types of longitudinal fold. Isostatic folds are broad folds that form in response to differential unloading of the footwalls of normal faults (Spencer, 1984; Wernicke and Axen, 1988; Buck, 1988) (Fig. 8). Whether footwall uplift reflects flexural processes or slip along spaced high-angle to vertical normal faults is controversial (Axen *et al.*, 1995; Manning and Bartley, 1994) but most workers agree that this mechanism has produced mountain-scale anticlines in the metamorphic core complexes of the North American cordillera and elsewhere. Isostatic folds can be distinguished from other longitudinal folds based on their large size and wide spacing, and because isostatic folding is the only mechanism that will fold normal faults about strike-parallel axes during slip on a single normal fault. Structurally deeper normal faults may fold overlying normal faults, however, and complicate the structural geometry (Gans *et al.*, 1985). The wavelengths of isostatic folds (10–50 km, John, 1987) exceed the wavelengths of all but the largest fault-bend folds.

Longitudinal fault-bend folds develop in the hanging walls of normal faults with changing dip-angles. 'Rollover fold' and 'reverse-drag fold' (Hamblin, 1965; Xiao and Suppe, 1992; Groshong, 1989, 1994) are the original terms used to describe these folds, but we prefer the fault-bend terminology when referring to the mechanism that produced the folds. The majority of fault-bend folds are relatively simple 'rollover' anticlines above listric normal faults. Since the recognition that some normal fault systems display ramp and flat geometries similar to those along thrust faults (Gibbs, 1984; McClay, 1989; Axen, 1993; Janecke *et al.*, 1996b), more complex folds are anticipated (Fig. 8). The size of fault-bend folds can vary over a broad range, depending on the size of the bend in the associated normal fault. Fault-bend folds can be distinguished from other longitudinal folds by the presence

of non-planar faults, and the absence of folding in the footwall (Xiao and Suppe, 1992). If non-rigid footwalls are present, as some have argued (Kilsdonk and Fletcher, 1989), then more complex hybrid types of folds may develop that are not easily distinguished from other types of longitudinal folds.

Fault-propagation folds, by analogy with contractional fault-propagation folds, form beyond the tiplines of faults (Fig. 8). Numerical modeling (Patton and Fletcher, 1995; Cooke and Pollard, 1997) and natural examples (Patton, 1984; Jackson and Leeder, 1994; Gawthorpe *et al.*, 1997; Gross *et al.*, 1997) suggest that normal faults project upward toward or up dip of the anticlinal flexure of the resultant monocline or anticline/syncline pair (Fig. 8). Distinguishing between longitudinal fault-bend and fault-propagation folds is based primarily on the presence of footwall folding and the geometric relationship between the fold and the normal fault. It may be difficult to interpret natural examples of fault-propagation folds where subsurface data or three-dimensional exposures are lacking. The size of a fault-propagation fold will depend on the size of the associated normal fault. Forced folds are a subset of fault-propagation folds in

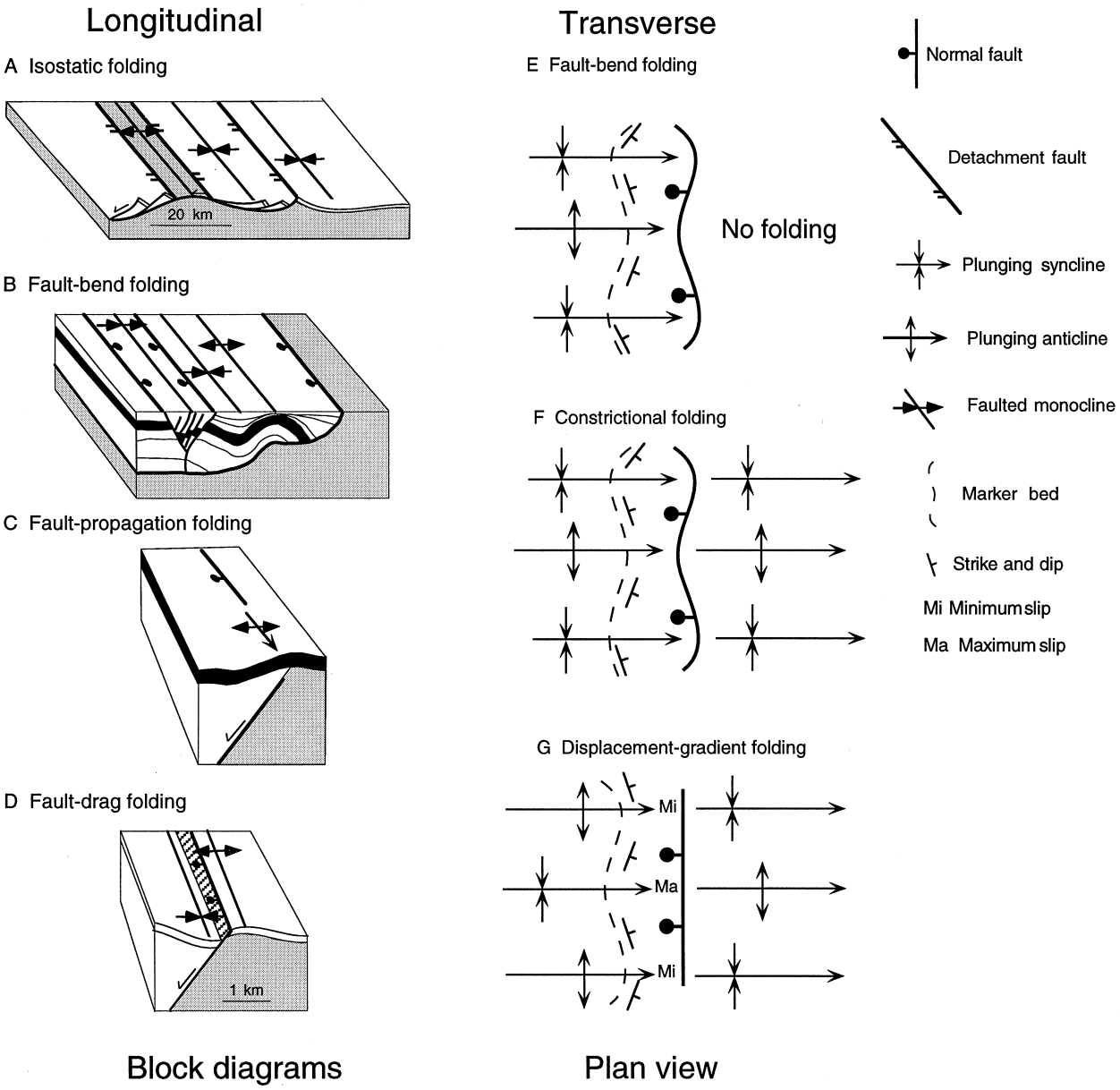

Fig. 8. Summary diagram of the mechanisms that produce the common types of longitudinal and transverse folds. Longitudinal folds are arranged by approximate size. Uppermost cross-section is modified from McClay (1989). The effect of normal faults besides those shown here are ignored. The rigidity of the footwall and hanging wall rocks is assumed to be similar in all cases except during fault-bend folding where the standard view of a rigid footwall was used (Suppe, 1983; Xiao and Suppe, 1992). Distinguishing between different types of folds is based on their overall size, orientation relative to the normal fault, shape of the normal fault, and whether the footwall is also folded.

which a faulted rigid substrate (basement) is overlain by an unfaulted stratified sequence (Chenet *et al*., 1987; Withjack *et al*., 1990; John and Howard, 1995; Howard and John, 1997; Gross *et al*., 1997).

Frictional resistance along fault planes has long been thought to produce localized fault-drag folds in the adjacent rocks (Fig. 8) (Twiss and Moores, 1992; Davis and Reynolds, 1996). Further study is needed, however, to determine whether the fault-drag folds of some workers are in fact breached fault-propagation folds, as some contend (Schlische, 1995). The distance between fault-drag folds and the associated normal fault is not quantified but folds are typically considered to be fault-drag folds if they are close to a normal fault. Thus they are among the smallest longitudinal folds and produce folds in both footwall and hanging wall rocks of similar rigidities.

Transverse folds

Common transverse folds include fault-bend folds, constrictional folds, and displacement-gradient folds (Table 1 and Fig. 8). Transverse fault-bend folds (fault-line deflection folds of Schlische, 1995) are associated with non-planar fault surfaces. Key characteristics of transverse fault-bend folds that distinguish them from constrictional folds and displacement-gradient folds include: no folding of footwall strata as long as the footwall rocks are more rigid than the hanging wall rocks, and the coincidence of folds in the hanging wall with transverse ramps in the adjacent normal fault (corrugations of some workers). If the footwall and hanging wall rocks have similar rigidities, a true fault-bend fold cannot develop and other mechanisms come into play. Along the simplest type of transverse fault-bend folds, synclines in the hanging wall develop adjacent to synformal parts of the fault (recesses) and anticlines develop adjacent to antiformal parts of the fault (salients) (Fig. 8), but geometries may vary as a function of the three-dimensional form of the fault. John (1987) showed that corrugations have wavelengths from 200 m to 10 km, amplitudes up to 400 m, and change in shape down the dip of the detachment fault in the Chemehuevi Mountains of the Colorado River extensional corridor.

Constrictional folds record horizontal shortening perpendicular to the regional extension direction (Fig. 8). Normal faults become folded during constrictional strain (Yin and Dunn, 1992; Mancktelow and Pavlis, 1994) and fold axes parallel the extension direction. Folds in the footwall and hanging wall of the fault are aligned and concordant. This characteristic easily distinguishes them from displacement-gradient folds (Fig. 8) which form along normal faults with significant slip-gradients (Schlische, 1993, 1995). Hanging-wall synclines produced by displacement gradients plunge toward the normal fault at the point of maximum slip and are along trend of gently plunging anticlines in the footwall where hanging wall and footwall rocks have a similar rigidity. Folds will be better developed in a less rigid fault block when the rigidity differs. Broad plunging synclines in the hanging wall of normal faults are the most common type of displacement-gradient folds (Schlische, 1993). Normal faults that produce displacement-gradient folds are not normally folded unless a second mechanism operates along the same or adjacent normal fault. In general, most types of transverse folds are more limited in their lateral extent than most types of longitudinal folds.

Oblique folds

Common oblique folds include fault-bend folds, transtensional folds and compound folds (Table 1). Fault-bend folds, like transverse fault-bend folds, reflect deformation of hanging wall rocks as they slip across non-planar fault surfaces and rigid footwall rocks. Corrugations on the faults are oblique to the overall strike of the normal fault, and neither the fault nor the footwall are folded in the process as long as the footwall is more rigid than the hanging wall. This mechanism may have produced folds in the Shadow Valley half graben of southeast California (Davis *et al*., 1993; Fowler *et al*., 1995; Friedmann *et al*., 1996).

Transtensional strain, like constrictional strain, will produce three-dimensional deformation. Shortening perpendicular to the finite extension axis is a natural consequence of this type of deformation and folds with axes parallel to the slip vector on normal-oblique faults are expected (Mancktelow and Pavlis, 1994; Harding *et al*., 1985). Transtensional folds are well-documented in the Death Valley region of California (Mancktelow and Pavlis, 1994; Holm *et al*., 1994). Diagnostic features of transtensional folds that distinguish them from fault-bend folds include: folded faults and footwall rocks, and fold axes that parallel the extension direction but are oblique to the strike of the normal-oblique faults. Because vertical axis rotation is common in transtensional environments, folds developed early in the deformation may not parallel younger folds (Mancktelow and Pavlis, 1994).

Compound folds are formed by more than one mechanism and may be longitudinal, transverse or oblique, depending on the mechanisms involved (Schlische, 1995). Oblique compound folds may develop where transverse and longitudinal mechanisms operate simultaneously along a single normal fault. In transverse accommodation zones, for example, where oppositely-dipping normal faults die out along strike, oblique anticlines connect the tips of normal faults that dip toward each other and oblique synclines connect the tips of normal faults that dip away from each other (Morley *et al.,* 1990; Olson, 1996; Faulds, 1996; Faulds and Varga, in press). We interpret the oblique anticlines as displacement-gradient anticlines at the fault tips superimposed on a roll-over anticlines above

two listric normal faults. The synclines are also formed by more than one process. Almost any combination of mechanisms is possible in nature, making compound folds potentially the most common type of extensional fold.

Other mechanisms, not included in Table 1, may produce locally plentiful folds in extending regions. These mechanisms include: forced (or drape) folding of layered sequences above faulted rigid substrates (Chenet *et al*., 1987; Withjack *et al*., 1990; John and Howard, 1995; Howard and John, 1997; Gross *et al*., 1997), secondary folding in the cores of larger structures (here called crowding structures), folding due to pluton emplacement (Lister and Baldwin, 1993) or differential compaction (Roberts and Yielding, 1991), and folding of basin-fill deposits beneath large rock avalanche and rock slide deposits (Boyer and Hossack, 1992).

PROCESSES OF FOLDING IN THE STUDY AREA

In our study area, as in many natural examples, it is hard to pin down the origin of individual folds. It is particularly difficult where a fold could be related to more than one normal fault (synclines A, I and G), where there is insufficient control on the subsurface geometry of the relevant normal faults (folds I, B, and C), where a train of parallel folds is present (anticline C and adjacent structures), or where more than one mechanism produced the final fold (anticline D) (Figs 2 & 4). Based on the criteria outlined in the previous section, we are fairly confident of the mechanisms that produced folds D, E, H, J, L, M, N and O. The origins of folds A, B, C, F, G, I and K are less certain.

The largest folds in the study area are the apparent rollover anticlines above listric normal faults (longitudinal fault-bend anticlines H, J and E). These anticlines produce intrabasinal structural highs that segment the rift basins into subbasins and locally expose pretectonic rocks. Anticline H, for example, which has a fold height of about 1.5 km, is such a large structure that it exposes a 3–7 km wide zone of Precambrian bedrock within the southeast Salmon rift basin (Fig. 3). Tertiary rocks to the east of the anticline are here interpreted as a subbasin of the larger Salmon rift basin, not as deposits of a distinct, unrelated depositional basin (e.g. Harrison, 1985). We interpret this NE- to NNE-trending anticline as a rollover anticline above a ramp in the NW- to W-dipping Agency–Yearian fault based on (1) the approximate parallelism of the fault and fold over a distance of more than 12 km (Fig. 3), (2) the large size of the anticline, and (3) its striking similarity to anticlines produced in sandbox models of extensional folds in the hanging walls of ramp-flat listric fault systems (Blankenau and Janecke, 1997; McClay, 1989). Two synclines southwest of anticline H (L and M) are probably also longitudinal fault-bend folds related to a ramp in the Agency–Yearian fault. The geometries of the once continuous synclines L and M are complicated by crosscutting faults and folds such as monocline K, anticline J, and the normal fault on the southwest flank of anticline J (Fig. 3).

Anticline J, which parallels and lies between two hanging wall strands of the Salmon basin detachment fault (Figs 3 & 6c), formed early in the history of this fault zone but after anticline H (Blankenau and Janecke, 1997). This large rollover anticline extends for about 10 km along trend and has a fold height of approximately 1 km (Fig. 6c). Figure 6(c), which reconstructs this rollover anticline prior to slip on a younger normal fault along its southwest flank, shows how similar the gross geometry of extensional and contractional folds can be. The southeast plunge of anticline J in the area of the cross section (Fig. 6c) is due to its position on the northwest flank of syncline M. The mechanism(s) that produced the longitudinal synclines NE and SW of anticline J (Figs 3 & 6c) is uncertain, but could include fault-bend, fault-drag, or fault-propagation folding. Longitudinal synclines in the immediate hanging walls of normal faults, like these, are very common in this region (Fig. 2b).

Several folds that are oblique to all the nearby normal faults result from multiple processes along one or more normal faults. Compound fold E, for example, is both a rollover fold in the hanging wall of the listric NW-dipping Little Eightmile Creek fault and a displacement-gradient anticline related to the northeastward decrease in slip across the fault (Figs 3, 4 & 6c,) (VanDenburg, 1997; VanDenburg *et al*., in press). We interpret anticline D as another compound fold resulting from rollover (longitudinal fault-bend folding) in the hanging walls of two strike-perpendicular listric normal faults; the NW-dipping Little Eightmile Creek and the west-dipping Maiden Peak faults (Figs 3 & 4). Because syncline A is oblique to both of the nearest normal faults (Lemhi Pass fault, Agency–Yearian fault, Figs 3 & 4) it is also likely to be a compound syncline. Transtension associated with the right-normal slip Lemhi Pass fault was of the wrong sense to produce this NNW-trending syncline.

Anticlines N and O in the eastern Medicine Lodge half graben (Fig. 2) are transverse fault-bends folds in the hanging wall of the upper detachment fault of the Muddy-Grasshopper detachment system (M'Gonigle, 1993; S. Janecke, unpublished data). Their east-plunging fold axes (Fig. 4) parallel the trend of, and project toward west-plunging corrugations in the underlying, generally west-dipping detachment fault. Anticline O (Fig. 7) has a smaller interlimb angle than the associated corrugation, perhaps due to tightening during a second episode of folding. The corrugations are major bends in the fault surface that are spaced about 2 km apart.

The origins of folds A, B, C, F, G, I and K are uncertain because more than one process could plausibly have given rise to them, or because no single mechanisms can account for all their characteristics. Further work, particularly in the footwalls of the normal faults, might clarify their origin. We do not know the origin of the train of oblique to nearly transverse folds parallel to anticline C (Fig. 3). The apparent absence of corrugations or true folds on the western strand of the Maiden Peak fault, directly east of the fold train (M'Gonigle and Hait, 1997) suggests that these folds are probably not transtensional or fault-bend folds. It seems equally unlikely that displacement gradients could produce the nine gentle folds in a N–S distance of only 7 km. The origin of anticline B, and the two small folds to the northwest, is also uncertain (Fig. 3) but might reflect transtension and/or displacement gradients along the low-angle Lemhi Pass fault.

Syncline G is a very broad, subtle, and isolated fold (Figs 3 & 4) that roughly parallels the underlying Maiden Peak fault to the east and the WSW-dipping Beaverhead normal fault to the west. Syncline G might be an isostatic syncline in the footwall of the Beaverhead fault but we cannot rule out a genetic relationship to the Maiden Peak fault because the fault may have been active in early Miocene to Recent time when syncline G formed (M'Gonigle, 1994; VanDenburg, 1997).

Syncline I plunges SE toward the Agency–Yearian normal fault but is also subparallel to the underlying Salmon basin–Lemhi Pass detachment fault (Fig. 3). The Agency–Yearian fault does not have a synclinal geometry in this area, nor is there evidence of synclinal folding in the footwall. The geometrical relationships are consistent with the syncline being a displacement-gradient fold related to the Agency–Yearian fault or a longitudinal fault-bend fold associated with the Salmon basin–Lemhi Pass detachment fault. If the latter interpretation is correct, there is a ramp on the Salmon basin–Lemhi Pass detachment fault in the subsurface near syncline I.

Monocline K is cut by a SW-dipping fault that parallels the fold axis, whereas anticline F plunges toward a small south-dipping normal fault (Fig. 3). Ambiguity about the sense of slip across the fault at monocline K complicates its interpretation.

The presence of fold-related growth strata associated with some of the folds in the study area (1) shows that extensional folding was coeval with normal faulting and (2) allowed us to discriminate between different mechanisms of folding (Blankenau and Janecke, 1997). Growth folds are best expressed in the southeast part of the Salmon basin but are also present in the Muddy Creek half graben (Janecke *et al*., in press) and possibly in the eastern half of the Horse Prairie rift basin. Folds H, M and L in the SE part of the Salmon basin exhibit changes in thickness, provenance and facies on opposite limbs of the folds. Equivalent strata are over three times as thick on the northwest limb of syncline M as on the SE limb, and display a pattern consistent with formation above a ramp in the underlying Agency–Yearian normal fault (Blankenau and Janecke, 1997; McClay, 1989). The sedimentary patterns indicate a hinge rolling to the northwest, and are therefore inconsistent with our initial interpretation of these folds as transverse fault-bend folds above a SW-plunging ridge in the underlying Salmon basin–Lemhi Pass fault system.

SIGNIFICANCE OF EXTENSIONAL FOLDS

Proper identification and interpretation of extensional folds is of utmost importance for structural and tectonic analyses. If extensional folds are misinterpreted, contraction may be inferred and the three-dimensional nature of the deformation may be overlooked. Criteria that distinguish extensional folds from contractional folds include: (1) a complete or near absence of reverse or thrust faults of the same age as the folds, (2) fold patterns that are inconsistent with formation in a fold and thrust belt, (3) a close spatial association between folds and normal faults, (4) cross-cutting relationships that show that normal faults and folds are the same age, and (5) growth strata that are consistent with deposition during extensional deformation.

When folds develop in a half graben, sedimentation patterns may be modified by the emerging highlands and basinal areas (Xiao and Suppe, 1992; Dorsey and Roberts, 1996; Dorsey and Becker, 1995; Gawthorpe *et al*., 1997; Blankenau and Janecke, 1997; Janecke *et al*., in press). In the syntectonic deposits of the Whipple Mountains metamorphic core complex, for example, changes in the thickness and facies of deposits reflect the presence of a rollover anticline and a large transverse anticline (Dorsey and Roberts, 1996; Dorsey and Becker, 1995). Field studies like these, theoretical modeling, and sandbox experiments, which show similar striking changes in sediment thickness across extensional folds (Xiao and Suppe, 1992; Ellis and McClay, 1988; McClay, 1989) raise the possibility that some of the sediment shed laterally from the footwalls of inferred cross faults in a rift zone (Fillmore, 1993; Nielson and Beratan, 1995; Friedmann and Burbank, 1995) may instead have had source areas at the crests of intrabasinal transverse or oblique extensional folds.

Folds provide structural traps in petroleum provinces and influence the availability of groundwater resources (Vogler and Robison, 1987; Rowan and Kligfield, 1989; Xiao and Suppe, 1992). The Ziana anticline in the northern Albuquerque basin of the Rio Grande rift, for example, brings a critical aquifer near enough to the surface to be a prime source of groundwater (W. Haneberg, personal communication, 1996).

Transverse and oblique folds are indicative of three-dimensional strain, a phenomenon that is increasingly being recognized in extending regimes (Anderson and Barnhard, 1993a,b; Duebendorfer and Simpson, 1994; Mancktelow and Pavlis, 1994; VanDenburg, 1997; VanDenburg *et al.*, in press). Three-dimensional strain may be relatively more common during extension than during contraction. The failure to recognize three-dimensional strain in extending regions can result in incorrect interpretations of the ancient state of stress, structural evolution, pre-extensional crustal structure, thickness and paleoelevations (Anderson and Barnhard, 1993; Mancktelow and Pavlis, 1994).

Extensional folds, being gentle to open, are often less conspicuous than folds that form in contraction, but are nonetheless important because they reflect processes of extension, influence the architecture of rift basins and provide strong evidence for three-dimensional strains. Extensional folds come in all sizes, ranging up to mountain scale and locally may have overturned limbs.

CONCLUSIONS

The view that folds require contraction is at odds with our discovery of more than 70 extensional folds in half graben of the Rocky Mountain Basin and Range province. Extensional folds are major structural features in these rift basins and even control the basic outlines of some of the basins. On a regional scale, the trends of most extensional folds are parallel or nearly perpendicular to the strikes of the largest normal faults. Most extensional folds trend NE–SW and SE–NW, but there is considerable variability in fold geometry across the region. Many folds in the study area form fold trains (more than two parallel folds). These are spaced up to 5 km apart, and lie both parallel and perpendicular to the associated normal fault. Interlimb angles of 15 selected folds range from 103° up to 175° (open to gentle folds) and average 141°. Plunges of the folds range from 01° to 46° and average 19°. Two small folds in the Medicine Lodge and Salmon half graben have locally overturned limbs.

At least three generations of folds are present, and they are genetically related to several generations of normal faults that extended the study area in both NE–SW and NW–SE directions during the Cenozoic. The intersection of orthogonal folds produced local dome and basin structures. Detailed mapping and structural analysis shows that from 30 to 45% of the hingelines and axes of the folds are oblique to the associated normal fault. This large number of oblique folds is puzzling because the best known types of extensional folds are longitudinal or transverse. An undocumented component of strike-slip deformation and/or multiple mechanisms of deformation could account for the large number of oblique folds. Whatever their origin, the abundant transverse and oblique folds result in a highly three-dimensional strain field.

Several different types of folds are present in the study area. We discriminate among the different possible types of folds based on the size of the folds, their orientation relative to the normal fault, whether the footwall was folded, the geometry of the normal fault, the concordance between footwall and hanging wall folds, and the presence and type of growth strata. We determine the origin of about half of the folds in our study population. The majority of these folds resulted from fault-bend folding processes and include both classic rollover anticlines, longitudinal synclines, and transverse to oblique anticlines and synclines. Several folds are oblique to all the nearby normal faults and were the product of multiple mechanisms and/or episodes of deformation.

Acknowledgements—This research was partially supported by NSF grant EAR 93-17395. Conversations with Michele Cooke, James Evans, Jeff Evans, James Faulds, Barbara John, John M'Gonigle and Terry Pavlis were helpful. The program Stereonet by Richard Allmendinger facilitated data analysis and presentation. This and an earlier version of the manuscript were improved by critical and helpful reviews by James Evans, James Faulds, Peter Hudleston, Mary Ford and Richard Groshong.

REFERENCES

Anderson, A. L. (1956) Geology and Mineral Resources of the Salmon Quadrangle, Lemhi County, Idaho. *Idaho Bureau of Mines and Geology Pamphlet* **106**.

Anderson, A. L. (1957) Geology and Mineral Resources of the Baker Quadrangle, Lemhi County, Idaho. *Idaho Bureau of Mines and Geology Pamphlet* **112,** 71 pp.

Anderson, A. L. (1961) Geology and Mineral Resources of the Lemhi Quadrangle, Lemhi County, Idaho. *Idaho Bureau of Mines and Geology Pamphlet* **124,** 111 pp.

Anderson, R. E. and Barnhard, T. P. (1993a) Aspects of three-dimensional strain at the margin of the extensional orogen, Virgin River depression area, Nevada, Utah, and Arizona. *Geological Society of America Bulletin* **105,** 1019–1052.

Anderson, R. E. and Barnhard, T. P. (1993b) Heterogeneous Neogene strain and its bearing on horizontal extension and horizontal and vertical contraction at the margin of the extensional orogen, Mormon Mountains area, Nevada and Utah. *U.S. Geological Survey Bulletin* **2011,** 44 pp.

Anderson, R. E., Barnhard, T. P. and Snee, L. W. (1994) Roles of plutonism, midcrustal flow, tectonic rafting, and horizontal collapse in shaping the Miocene strain field of the Lake Mead area, Nevada and Arizona. *Tectonics* **13,** 659–674.

Axelrod, R. B. (1984) Tertiary sedimentary facies, depositional environments, and structure, Jefferson Basin, southwest Montana. M.Sc. thesis. University of Montana.

Axen, G. J. (1993) Ramp-flat detachment faulting and low-angle normal reactivation of the Tule Springs thrust, southern Nevada. *Geological Society of America Bulletin* **105,** 1076–1090.

Axen, G. J., Bartley, J. M. and Selverstone, J. (1995) Structural expression of a rolling hinge in the footwall of the Brenner Line normal fault, eastern Alps. *Tectonics* **14,** 1380–1392.

Bartley, J. M., Fletcher, J. M. and Glazner, A. F. (1990) Tertiary extension and contraction of lower-plate rocks in the central Mojave metamorphic core complex, southern California. *Tectonics* **9,** 521–534.

Black, B. A. and Hiss, W. L. (1974) Structure and stratigraphy in the vicinity of the Shell Oil Co. Santa Fe Pacific No. 1 test well, southern Sandoval County, New Mexico. In *Ghost Ranch*, ed. C.

T. Siemers, pp. 365–370. New Mexico Geological Society 25th Field Conference Guidebook.
Blankenau, J. J. and Janecke, S. U. (1997) Three-dimensional structure of a Paleogene rift basin and its effects on synextensional sedimentation, Salmon basin ID. *Geological Society of America Abstracts with Programs* **29,** 221.
Boyer, S. E. and Hossack, J. R. (1992) Structural features and emplacement of surficial gravity-slide sheets, northern Idaho–Wyoming thrust belt. In *Regional Geology of Eastern Idaho and Western Wyoming*, eds P. K. Link, M. A. Kuntz and L. B. Platt, pp. 197–214. Geological Society of America Memoir, **179**.
Bryant, B. (1990) Geologic map of the Salt Lake City $30' \times 60'$ Quadrangle, north-central Utah, and Uinta County, Wyoming. *U.S. Geological Survey* **I-1944** (scale 1:100 000).
Buck, W. R. (1988) Flexural rotation of normal faults. *Tectonics* **7,** 959–974.
Burton, S. M. (1973) Structural geology of the northern part of Clarkston Mountain, Malad Range, Utah–Idaho. M.Sc. thesis. Utah State University.
Byers, F. M., Jr (1960) Geology of the Alvord Mountain quadrangle, San Bernadino County, California. *U.S. Geological Survey Bulletin* **1089-A** (scale 1:62 500).
Chenet, P. Y., Colletta, B., Letouzey, J., Desforges, G., Ousset, E. and Zaghloul, E. A. (1987) Structures associated with extensional tectonics in the Suez rift. In *Continental Extensional Tectonics*, eds M. P. Coward, J. F. Dewey and P. L. Hancock, pp. 551–558. Special Publication of the Geological Society of London, **28**.
Compton, R. R. (1972) Geologic map of the Yost Quadrangle, Box Elder County, Utah and Cassia County, Idaho. *U.S. Geological Survey Miscellaneous Investigations Map* **I-672** (scale 1:31 680).
Compton, R. R. (1975) Geologic map of the Park Valley Quadrangle, Box Elder County, Utah, and Cassia County, Idaho. *U.S. Geological Survey Miscellaneous Investigations Map* **I-873** (scale 1:31 680).
Compton, R. R. (1983) Displaced Miocene rocks on the west flank of the Raft River-Grouse Creek core complex, Utah. In *Tectonics and Stratigraphic Studies in the Eastern Great Basin*, eds D. M. Miller, V. R. Todd and K. A. Howard, pp. 271–280. Geological Society of America Memoir, **157**.
Compton, R. R., Todd, V. R., Zartman, R. E. and Naeser, C. W. (1977) Oligocene and Miocene metamorphism, folding, and low-angle faulting in northwestern Utah. *Geological Society of America Bulletin* **88,** 1237–1250.
Constenius, K. N. (1996) Late Paleogene extensional collapse of the Cordilleran foreland fold and thrust belt. *Geological Society of America Bulletin* **108,** 20–39.
Cooke, M. and Pollard, D. (1997) Bedding plane slip in initial stages of fault-related folding. *Journal of Structural Geology* **19,** 567–581.
Coppinger, W. (1974) Stratigraphic and structural study of belt Supergroup and associated rocks in a portion of the Beaverhead Mountains, southwest Montana, and east-central Idaho. Ph.D. dissertation. Miami University.
Crone, A. J. and Haller, K. M. (1991) Segmentation and coseismic behavior of Basin and Range normal faults: Examples from east-central Idaho and southwestern Montana, U.S.A. *Journal of Structural Geology* **13,** 151–164.
Davis, G. A., Fowler, T. K., Bishop, K. M., Brudos, T. C., Friedmann, S. J., Burbank, D. W., Parke, M. A. and Burchfiel, B. C. (1993) Pluton pinning of an active Miocene detachment fault system, eastern Mojave Desert, California. *Geology* **21,** 627–630.
Davis, G. H. and Reynolds, S. J. (1996) *Structural Geology of Rocks and Regions*. John Wiley and Sons, Inc.
Dickinson, W. R. (1991) Tectonic Setting of Faulted Tertiary Strata Associated with the Catalina Core Complex in Southern Arizona. *Geological Society of America Special Paper* **264,** 106 pp.
Dorsey, R. J. and Becker, U. (1995) Evolution of a large Miocene growth structure in the upper plate of the Whipple detachment fault, northeastern Whipple Mountains, California. *Basin Research* **7,** 151–163.
Dorsey, R. J. and Roberts, P. (1996) Evolution of the Miocene north Whipple Basin in the Aubrey Hills, western Arizona, upper plate of the Whipple detachment fault. In *Reconstructing the History of Basin and Range Extension Using Sedimentology and Stratigraphy*, ed. K. K. Beratan, pp. 127–146. Geological Society of America Special Paper, **303**.
Dubois, D. P. (1982) Tectonic framework of basement thrust terrane, northern Tendoy Range, Southwest Montana. In *Geologic Studies in the Cordilleran Thrust Belt*, ed. R. B. Powers, pp. 145–158. Rocky Mountain Association of Geologists.
Duebendorfer, E. M. and Simpson, D. A. (1994) Kinematics and timing of Tertiary extension in the western Lake Mead region, Nevada. *Geological Society of America Bulletin* **106,** 1057–1073.
Dula, W. F. (1991) Geometric models of listric normal faults and rollover folds. *American Association of Petroleum Geologists Bulletin* **75,** 1609–1625.
Ellis, P. G. and McClay, K. R. (1988) Listric extensional fault systems—results of analogue model experiments. *Basin Research* **1,** 55–70.
Faulds, J. E. (1996) Geologic map of the Fire Mountain quadrangle Nevada and Arizona. *Nevada Bureau of Mines and Geology Map* **106** (scale 1:24 000).
Faulds, J. E. and Varga, R. J. (in press) The role of accommodation zones and transfer zones in the regional segmentation of extended terranes. In *Accommodation Zones and Transfer Zones: Regional Segmentation of the Basin and Range Province*, eds J. E. Faulds and J. H. Stewart. Geological Society of America Special Paper.
Faulds, J. E., Feuerbach, D. L., Reagan, M. K., Metcalf, R. V., Gans, P. and Walker, J. D. (1995) The Mt Perkins block, northwestern Arizona: An exposed cross section of an evolving, pre- to syn-extensional magmatic system. *Journal of Geophysical Research* **100,** 15249–15266.
Faulds, J. E., Geissman, J. W. and Mawer, C. K. (1990) Structural development of a major extensional accommodation zone in the Basin and Range Province, northwestern Arizona and southern Nevada; Implications for kinematic models of continental extension. In *Basin and Range Extensional Tectonics Near the Latitude of Las Vegas, Nevada*. ed. B. P. Wernicke. Geological Society of America Memoir, **176,** pp. 37–76.
Fillmore, R. B. (1993) Sedimentation and extensional basin evolution in a Miocene metamorphic core complex setting, Alvord Mountain, central Mojave Desert, California, U.S.A. *Sedimentology* **40,** 721–742.
Fowler, T. K., Jr, Friedmann, S. J., Davis, G. A. and Bishop, K. M. (1995) Two-phase evolution of the Shadow Valley Basin, southeastern California: A possible record of footwall uplift during extensional detachment faulting. *Basin Research* **7,** 165–179.
Friedmann, S. J. and Burbank, D. W. (1995) Rift basins and supradetachment basins: Intracontinental extensional end-members. *Basin Research* **7,** 109–127.
Friedmann, S. J., Davis, G. A. and Fowler, T. K. (1996) Geometry, paleodrainage, and geologic rates from the Miocene Shadow Valley supradetachment basin, eastern Mojave Desert, California. In *Reconstructing the History of Basin and Range Extension Using Sedimentology and Stratigraphy*, ed. K. K. Beratan, pp. 85–106. Geological Society of America Special Paper, **303**.
Gans, P. B., Miller, E. L., McCarthy, J. and Ouldcott, M. L. (1985) Tertiary extensional faulting and evolving ductile–brittle transition zones in the northern Snake Range and vicinity: New insights from seismic data. *Geology* **13,** 189–193.
Gawthorpe, R. L., Sharp, I., Underhill, J. R. and Gupta, S. (1997) Linked sequence stratigraphic and structural evolution of propagating normal faults. *Geology* **25,** 795–798.
Gibbs, A. D. (1984) Structural evolution of extensional basin margins. *Journal of the Geological Society of London* **141,** 609–620.
Gordon, I. and Heller, P. L. (1993) Evaluating major controls on basinal stratigraphy, Pine Valley, Nevada: Implications for syntectonic deposition. *Geological Society of America Bulletin* **105,** 47–55.
Gray, W. E. (1975) Structural geology of the southern part of Clarkston Mountain, Malad Range, Utah. M.Sc. thesis. Utah State University.
Groshong, R. H., Jr (1989) Half-graben structures: Balanced models of extensional fault-bend folds. *Geological Society of America Bulletin* **101,** 96–105.
Groshong, R. H., Jr (1994) Area balance, depth to detachment, and strain in extension. *Tectonics* **13,** 1488–1497.
Gross, M. R., Becker, A. and Gutiérrez-Alonso, G. (1997) Transfer of displacement from multiple slip zones to a major detachment in an extensional regime: Example from the Dead Sea rift, Israel. *Geological Society of America Bulletin* **109,** 1021–1035.
Hamblin, W. K. (1965) Origin of "reverse drag" on the downthrown side of normal faults. *Geological Society of America Bulletin* **76,** 1145–1164.

Harding, T. P., Vierbuchen, R. C. and Christie-Blick, N. (1985) Structural styles, plate-tectonic settings, and hydrocarbon traps of divergent (transtensional) wrench faults. In *Strike-Slip Deformation, Basin Formation, and Sedimentation*, eds K. T. Biddle and N. Christie-Blick, pp. 51–78. Social and Economic Paleontologists and Mineralogists Special Publication, **37**.

Harms, T. A. and Price, R. A. (1992) The Newport fault: Eocene listric normal faulting, mylonitization, and crustal extension in northeast Washington and northwest Idaho. *Geological Society of America Bulletin* **104,** 745–761.

Harrison, S. (1985) Sedimentology of Tertiary rocks near Salmon Idaho. Ph.D. dissertation. University of Montana.

Holm, D. K., Fleck, R. J. and Lux, D. R. (1994) The Death Valley Turtlebacks reinterpreted as Miocene–Pliocene folds of a major detachment surface. *Journal of Geology* **102,** 718–727.

Hopkins, D. L. (1982) A structural study of the Durst Mountain and north central Wasatch Mountains, Utah. M.Sc. thesis, University of Utah.

Howard, K. A. and John, B. E. (1997) Fault-related folding during extension: Plunging basement-cored folds in the Basin and Range. *Geology* **25,** 223–226.

Jackson, J. and Leeder, M. R. (1994) Drainage systems and the development of normal faults: An example from Pleasant Valley Nevada. *Journal of Structural Geology* **16,** 1041–1059.

Janecke, S. U. (1992a) Geologic map of the Donkey Hills and part of the Doublesprings 15′ quadrangles, Custer and Lemhi Counties, Idaho. *Idaho Geological Survey Technical Report*. **92–47** (Scale 1:62 500).

Janecke, S. U. (1992b) Geologic map of the northern two-thirds of the Methodist Creek and Mackay and some of the Mackay Reservoir and Sunset Peak 7.5′ quadrangles, Custer and Butte Counties, Idaho. *Idaho Geological Survey Technical Report* **92–81,** (scale 1:24 000).

Janecke, S. U. (1995) Eocene to Oligocene half grabens of east-central Idaho: Structure, stratigraphy, age and tectonics. *Northwest Geology* **24,** 159–199.

Janecke, S. U., Blankenau, J. J. and VanDenburg, C. J. (1996a) Extensional folds: Their classification and significance. *Geological Society of America Abstracts with Programs* **28,** 115.

Janecke, S. U., Perry, W. J. and M'Gonigle, J. W. (1996b) Scale dependent reactivation of pre-existing structures by an Eocene-Oligocene detachment fault, southwestern Montana. *Geological Society of America Abstracts with Programs* **28,** 78.

Janecke, S. U., McIntosh, W. and Good, S. (in press) Structure and stratigraphy of a temperate Eocene–Oligocene supra-detachment basin, Muddy Creek half graben, southwest Montana: testing supradetachment basin models. *Basin Research*.

John, B. E. (1987) Geometry and evolution of a mid-crustal extensional fault system: Chemehuevi Mountains, southeastern California. In *Continental Extensional Tectonics*, eds M. P. Coward, J. F. Dewey and P. L. Hancock, pp. 313–336. Special Publication of the Geological Society of London, **28**.

John, B. E. and Howard, K. A. (1995) Field Trip 6: Disharmonic drape folds in the highly attenuated Colorado River extensional corridor, California and Arizona. In *Geological Investigations of an Active Margin*. eds S. F. McGill and T. M. Ross, pp. 94–106. Geological Society of America.

Kelley, V. C. (1977) Geology of Albuquerque Basin, New Mexico. *New Mexico Bureau of Mines & Mineral Resources Memoir* **33,** 59.

Kellogg, K. S., Schmidt, C. J. and Young, S. W. (1995) Basement and cover-rock deformation during Laramide contraction in the northern Madison Range (Montana) and its influence on Cenozoic basin formation. *American Association of Petroleum Geologists Bulletin* **79,** 1117–1137.

Kilsdonk, B. and Fletcher, R. C. (1989) An analytical model of hanging-wall and footwall deformation at ramps on normal faults and thrusts. *Tectonophysics* **163,** 153–168.

Kruger, J. M., Johnson, R. A. and Houser, B. B. (1995) Miocene–Pliocene half-graben evolution, detachment faulting and late-stage core complex uplift from reflection seismic data in south-east Arizona. *Basin Research* **7,** 129–149.

Kuenzi, W. D. and Fields, R. W. (1971) Tertiary stratigraphy, structure, and geologic history, Jefferson basin, Montana. *Geological Society of American Bulletin* **82,** 3374–3394.

Lewis, C. J. and Baldridge, W. S. (1994) Crustal extension in the Rio Grande rift, New Mexico: Half-grabens, accommodation zones, and shoulder uplifts in the Ladron Peak–Sierra Lucero area. In *Basins of the Rio Grande Rift: Structure, Stratigraphy, and Tectonic Setting*. eds G. R. Keller and S. M. Cather, pp. 135–155. Geological Society of America Special Paper, **291**.

Liberty, L. M., Heller, P. L. and Smithson, S. B. (1994) Seismic reflection evidence for two-phase development of Tertiary basins from east-central Nevada. *Geological Society of America Bulletin* **106,** 1621–1633.

Link, P. K. (1982a) Geology of the upper Proterozoic Pocatello Formation, Bannock Range, southeastern Idaho. Ph.D. dissertation. University of California Santa Barbara.

Link, P. K. (1982b) Structural Geology of the Oxford Peak and Malad Summit quadrangles, Bannock Range, southeastern Idaho. In *Geologic Studies of the Cordilleran Thrust Belt*, ed. R. B. Powers, pp. 851–858. Rocky Mountain Association of Geologists.

Lister, G. S. and Baldwin, S. L. (1993) Plutonism and the origin of metamorphic core complexes. *Geology* **21,** 607–610.

Livaccari, R. F., Geissman, J. W. and Reynolds, S. J. (1995) Large-magnitude extensional deformation in the South Mountains metamorphic core complex, Arizona: Evaluation with paleomagnetism. *Geological Society of America Bulletin* **107,** 877–894.

M'Gonigle, J. and Hait, M. H. J. (1997) Geologic map of the Jeff Davis Peak Quadrangle and the eastern part of the Everson Creek Quadrangle, Beaverhead County, SW Montana. *U.S. Geological Survey Geological Investigations Map* **I-2604** (scale 1:24 000).

M'Gonigle, J. W. (1993) Geologic map of the Medicine Lodge Peak quadrangle, Beaverhead County, Southwest Montana. *U.S. Geological Survey Geologic Quadrangle Map* **GQ-1724** (scale 1:24 000).

M'Gonigle, J. W. (1994) Geologic map of the Deadman Pass quadrangle, Beaverhead county, southwest Montana. *U.S. Geological Survey Quadrangle Map* **GQ-1753** (scale 1:24 000).

M'Gonigle, J. W. and Dalrymple, G. B. (1993) $^{40}Ar/^{39}Ar$ ages of Challis volcanic rocks and the initiation of Tertiary sedimentary basins in southwestern Montana. *Mountain Geologist* **30,** 112–118.

M'Gonigle, J. W. and Dalrymple, G. B, (1996) $^{40}Ar/^{39}Ar$ ages of some Challis Volcanic Group rocks and the initiation of Tertiary sedimentary basins in southwestern Montana. *U.S. Geological Survey Bulletin* **2132,** 17 pp.

M'Gonigle, J. W., Kirschbaum, M. A. and Weaver, J. N. (1991) Geologic map of the Hansen Ranch quadrangle, Beaverhead county, southwest Montana. *U.S. Geological Survey Geological Quadrangle Map* **GQ 1704,** (scale 1:24 000).

Mancktelow, N. S. and Pavlis, T. L. (1994) Fold-fault relationships in low-angle detachment systems. *Tectonics* **13,** 668–685.

Manning, A. H. and Bartley, J. M. (1994) Postmylonitic deformation in the Raft River metamorphic core complex, northwestern Utah: Evidence of a rolling hinge. *Tectonics* **13,** 596–612.

May, S. J. and Russell, L. R. (1994) Thickness of the syn-rift Santa Fe Group in the Albuquerque Basin and its relation to structural style. In *Basins of the Rio Grande Rift: Structure, Stratigraphy, and Tectonic Setting*, eds G. R. Keller and S. M. Cather, pp. 113–124. Geological Society of America Special Paper, **291**.

Mayer, J. N. (1979) Structural geology of the northern part of Oxford Quadrangle, Idaho. M.Sc. thesis. Utah State University.

McClay, K. R. (1989) Physical models of structural styles during extension. In *Extensional Tectonics and Stratigraphy of the North Atlantic Margins*, eds A. J. Tankard and H. R. Balkwill, pp. 95–110. American Association of Petroleum Geologists Memoir, **46**.

Miller, D. A. and Schneyer, J. D. (1994) Geologic map of the Sunset Pass quadrangle, Box Elder County, Utah. *Utah Geological Survey Map* **154** (scale 1:24 000).

Mohapatra, G. K. and Johnson, R. A. (1995) 3-D constraints on Neogene deformation in the Great Salt Lake basin, from fault-plane and hanging wall geometries. *EOS Transactions F577* **76,** 576–577.

Morley, C. K., Nelson, R. A., Patton, T. L. and Munn, S. G. (1990) Transfer zones in the East African rift system and their relevance to hydrocarbon exploration in rifts. *American Association of Petroleum Geologists Bulletin* **74,** 1234–1253.

Mullens, T. E. and Izett, G. A. (1963) Geology of the Paradise quadrangle, Utah. *U.S. Geological Survey Geologic Quadrangle Map* **GQ-185** (scale 1:24 000).

Naruk, S. J., Bykerk-Kaufman, A., Currier-Lewis, D., Davis, G. H., Faulds, J. E. and Lewis, S. W. (1986) Kink folding in an extended terrane: Tortilla Mountains southeastern Arizona. *Geology* **14,** 1012–1015.

Nielson, J. E. and Beratan, K. K. (1995) Stratigraphic and structural synthesis of a Miocene extensional terrane, southeast California and west-central Arizona. *Geological Society of America Bulletin* **107,** 241–252.

Olson, E. L. (1996) Geometry and kinematics of an extensional anticline, Highland Spring Range, southern Nevada. M.Sc. thesis. University of Iowa.

Oriel, S. S. and Platt, L. B. (1980) Geologic map of the Preston $1^\circ \times 2^\circ$ quadrangle, south-eastern Idaho and western Wyoming. *U.S. Geological Survey Map* **I-1127** (scale 1:250 000).

Oviatt, C. G. (1986a) Geologic map of the Cutler Dam Quadrangle, Box Elder and Cache Counties, Utah. *Utah Geological and Mineral Survey Map* **91** (scale 1:24 000).

Oviatt, C. G. (1986b) Geologic map of the Honeyville Quadrangle, Box Elder and Cache Counties, Utah. *Utah Geological and Mineral Survey Map* **88** (scale 1:24 000).

Patton, T. L., III (1984) Normal-fault and fold development in sedimentary rocks above a pre-existing basement normal fault. Ph.D. dissertation. Texas A&M University.

Patton, T. L., III and Fletcher, R. C. (1995) Mathematical block-motion model for deformation of a layer above a buried fault of arbitrary dip and sense of slip. *Journal of Structural Geology* **17,** 1455–1472.

Ramsay, J. G. and Huber, M. I. (1987) The techniques of modern structural geology. In *Folds and Fractures*, Academic Press, **2**.

Roberts, A. M. and Yielding, G. (1991) Deformation around basin-margin faults in the North Sea/mid-Norway rift. In *The Geometry of Normal Faults*. eds A. M. Roberts, G. Yielding and B. Freeman, pp. 61–78. Geological Society of London Special Publication, **56**.

Rowan, M. G. and Kligfield, R. (1989) Cross section restoration and balancing as aid to seismic interpretation of extensional terranes. *American Association of Petroleum Geologists Bulletin* **73,** 955–966.

Russell, L. R. and Snelson, S. (1994) Structure and tectonics of the Albuquerque Basin segment of the Rio Grande rift: Insights from reflection seismic data. In *Basins of the Rio Grande Rift: Structure, Stratigraphy, and Tectonic Setting*, eds G. R. Keller and S. M. Cather, pp. 83–112. Boulder, Colorado, **291**.

Sacks, P. E. and Platt, L. B. (1985) Depth and timing of decollement extension, southern Portneuf range, southeastern Idaho. In *Orogenic Patterns and Stratigraphy of North-Central Utah and Southeastern Utah*, eds G. J. Kerns and R. L. Kerns Jr, pp. 119–127. Utah Geological Association Publication, **14**.

Schlische, R. W. (1993) Anatomy and evolution of the Triassic–Jurassic continental rift system, eastern North America. *Tectonics* **12,** 1026–1042.

Schlische, R. W. (1995) Geometry and origin of fault-related folds in extensional settings. *American Association of Petroleum Geologists Bulletin* **79,** 1661–1678.

Schmidt, E. A. (1971) A structural investigation of the northern Tortilla mountains, Pinal Co., Arizona. Ph.D. dissertation. University of Arizona.

Scholten, R. and Ramspott, L. D. (1968) Tectonic mechanisms indicated by structural framework of central Beaverhead Range, Idaho-Montana. *Geological Society of America Special Paper* **104,** 70 pp.

Smith, K. A. (1997) Stratigraphy, geochronology, and tectonics of the Salt Lake Formation (Tertiary) of southern Cache Valley, Utah. M.Sc. thesis. Utah State University.

Smith, K. A., Kirchner, B. T. and Oaks, R. Q., Jr (1994) Evidence of two episodes of quiescence plus possible compressional tectonism during late Cenozoic deposition of the Salt Lake Formation, Cache Valley, N-central Utah, USA. *Geological Society of America Abstracts with Program* **26,** 64.

Smith, K. A., Oaks, R. Q., Jr and Janecke, S. U. (1997) N-trending folds and ENE-striking normal faults postdate 5.1 Ma Salt Lake Formation and predate pediment, Cache Valley, Utah, NE Basin-and-Range province. *Geological Society of America Abstracts with Programs* **29,** 115.

Spencer, J. E. (1984) Role of tectonic denudation in warping and uplift of low-angle normal faults. *Geology* **12,** 95–98.

Spencer, J. E. and Reynolds, S. J. (1991) Tectonics of mid-Tertiary extension along a transect through west-central Arizona. *Tectonics* **10,** 1204–1221.

Stewart, J. H., Anderson, R. E., Beard, L. S., Billingsley, G. H., Cather, S. M., Dilles, J. H., Dokka, R. K., Faulds, J. E., Grose, T. L. T., Henry, C. D., Janecke, S. U., Miller, D. M., Richard, S. M., Roldan-Quintana, J., Scott, R. B., Sears, J. W. and Williams, V. S. (in press) Map showing Cenozoic tilt domains and associated structural features, western North America. In *Accommodation Zones and Transfer Zones: Regional Segmentation of the Basin and Range Province*, eds J. E. Faulds and J. H. Stewart. Geological Society of America Special Paper.

Stewart, J. H. and Diamond, D. S. (1990) Changing patterns of extensional tectonics; Overprinting of the basin of the middle and upper Miocene Emerald Formation in western Nevada by younger structural basins. In *Basin and Range Extensional Tectonics Near the Latitude of Las Vegas, Nevada*, ed. B. P. Wernicke, pp. 447–476. Geological Society of America Memoir, **176**.

Suppe, J. (1983) Geometry and kinematics of fault-bend folding. *American Journal of Science* **283,** 684–721.

Taylor, W. J. (1990) Spatial and temporal relations of Cenozoic volcanism and extension in the North Pahroc and Seaman Ranges, eastern Nevada. In *Basin and Range Extensional Tectonics Near the Latitude of Las Vegas, Nevada*, ed. B. P. Wernicke, pp. 181–194. Geological Society of America Memoir, **176**.

Twiss, R. J. and Moores, E. M. (1992) *Structural Geology*. Freeman and Co.

VanDenburg, C. J. (1997) Tectonic and paleogeographic evolution of the Horse Prairie half graben, southwest Montana. M.Sc. thesis. Utah State University.

VanDenburg, C. J., Janecke, S. U. and McIntosh, W. C. (in press) Three-dimensional strain produced by >50 m.y. of episodic extension, Horse Prairie basin area, SW Montana, U.S.A. *Journal of Structural Geology*.

Vogler, H. A. and Robison, B. A. (1987) Exploration for deep geopressured gas: Corair trend, offshore trend, offshore Texas. *American Association of Petroleum Geologists Bulletin* **71,** 777–787.

Wernicke, B. P. and Axen, G. J. (1988) On the role of isostasy in the evolution of normal fault systems. *Geology* **16,** 848–851.

Willard, P. D. (1972) Tertiary igneous rocks of northeastern Cache Valley, Idaho. M.Sc. thesis. Utah State University.

Withjack, M. O., Olson, J. and Oeterson, E. (1990) Experimental models of extensional forced folds. *American Association of Petroleum Geologists Bulletin* **74,** 1038–1054.

Xiao, H. and Suppe, J. (1992) Origin of rollover. *America Association of Petroleum Geologists Bulletin* **76,** 509–529.

Yin, A. (1991) Mechanisms for the formation of the domal and basinal detachment faults: a three-dimensional analysis. *Journal of Geophysical Research* **96,** 14577–14594.

Yin, A. and Dunn, J. F. (1992) Structural and stratigraphic development of the Whipple–Chemehuevi detachment fault system, southeastern California: Implications for the geometrical evolution of domal and basinal low angle normal faults. *Geological Society of America Bulletin* **104,** 659–674.

APPENDIX SOURCES OF DATA FOR FIG. 1

1—Harms and Price (1992); 2—Kuenzi and Fields (1971); Axelrod (1984); 3—Anderson (1956, 1957, 1961); J. Blankenau, and S. U. Janecke unpublished mapping, 1994-1997; 4—Coppinger (1974); S. U. Janecke, J. M'Gonigle and W. Perry Jr., unpublished mapping; 5—VanDenburg (1997); M'Gonigle and Hait (1997); 6—Dubois (1982); M'Gonigle *et al.* (1991); M'Gonigle (1993); S. U. Janecke, unpublished mapping, 1996; 7—Kellogg *et al.* (1995); 8—S. U. Janecke, unpublished mapping, 1995; 9—Scholten and Ramspott (1968); Crone and Haller (1991); 10—Janecke (1992a, 1995); 11—Janecke (1992b, 1995); 12—Oriel and Platt (1980); Sacks and Platt (1985); 13—Mayer (1979); Link (1982a and b); 14—Willard (1972); Oriel and Platt (1980); 15—Burton (1973); S. U. Janecke, unpublished mapping, 1997; 16—Gray (1975); Oviatt (1986a, b); M. Swenson, K. Goessel, R. Oaks and S. Janecke, unpublished mapping, 1996; 17—Smith *et al.* (1994, 1997); Smith (1997), R. Q. Oaks, unpublished mapping, 1995; Mullens and Izett (1963); 18—Miller and Schneyer (1994); 19—Compton (1972, 1975); Compton *et al.* (1977); 20—Compton (1983); 21—Hopkins (1982); Bryant (1990); 22—Mohapatra and Johnson (1995); Constenius (1996); 23—D. Miller, personal communication, 1995; 24—Gordon and Heller (1993); 25—Liberty *et al.* (1994); 26—Anderson and Barnard (1993a,

b); Anderson *et al*. (1994); 27—Taylor (1990); 28—Stewart and Diamond (1990); 29—Mancktelow and Pavlis (1994); Holm *et al*. (1994); 30—Fowler *et al*. (1995); Friedmann and Burbank (1995); 31—Faulds (1996); Faulds *et al*. (1990, 1995); Olson (1996); Faulds and Varga (in press); 32—Byers (1960); Fillmore (1993); 33—Spencer (1984); John (1987); Spencer and Reynolds (1991); Yin (1991); Yin and Dunn (1992); 34—Dorsey and Becker (1994); John and Howard (1995); Dorsey and Roberts (1996); Howard and John (1997); 35—Livaccari *et al*. (1995); 36—Schmitt (1971); Naruk *et al*. (1986); Dickinson (1991); 37—Kruger *et al*. (1995); 38—Lewis and Baldridge (1994); 39—Black and Hiss (1974); Kelley (1977); May and Russell (1994).